Published in final edited form as:
J Bone Miner Res. 2012 September ; 27(9): 2001–2014. doi:10.1002/jbmr.1663.

PTH Induces Differentiation of Mesenchymal Stem Cells by Enhancing BMP Signaling

Bing Yu[1], **Xiaoli Zhao**[2], **Chaozhe Yang**[3], **Janet Crane**[4], **Lingling Xian**[1], **William Lu**[2], **Mei Wan**[1], and **Xu Cao**[1,*]

[1]Department of Orthopaedic Surgery, Johns Hopkins University School of Medicine, Baltimore, MD, USA

[2]Department of Orthopaedics and Traumatology, University of Hong Kong, Hong Kong, China

[3]Center for Clinical and Community Research, Children's National Medical Center, Washington, DC, USA

[4]Department of Pediatrics, Johns Hopkins University School of Medicine, Baltimore, MD, USA

Abstract

Parathyroid hormone (PTH) stimulates bone remodeling and induces differentiation of bone marrow mesenchymal stromal/stem cells (MSCs) by orchestrating activities of local factors such as bone morphogenetic proteins (BMPs). The activity and specificity of different BMP ligands are controlled by various extracellular antagonists that prevent binding of BMPs to their receptors. Low-density lipoprotein receptor-related protein 6 (LRP6) has been shown to interact with both the PTH and BMP extracellular signaling pathways by forming a complex with PTH1R and sharing common antagonists with BMPs. We hypothesized that PTH-enhanced differentiation of MSCs into the osteoblast lineage through enhancement of BMP signaling occurs by modifying the extracellular antagonist network via LRP6. *In vitro* studies using multiple cell lines, including Sca-1^{+}CD45^{-}CD11b^{-} MSCs showed that a single injection of PTH enhanced phosphorylation of Smad1 and could also antagonize the inhibitory effect of noggin. PTH treatment induced endocytosis of a PTH1R/LRP6 complex and resulted in enhancement of phosphorylation of Smad1 that was abrogated by deletion of PTH1R, β-arrestin, or chlorpromazine. Deletion of LRP6 alone lead to enhancement of pSmad1 levels that could not be further increased with PTH treatment. Finally, knockdown of LRP6 increased the exposure of endogenous cell-surface BMPRII significantly in C2C12 cells and PTH treatment significantly enhanced cell surface binding of ^{125}I-BMP2 in a dose- and time-dependent manner, implying that LRP6 organizes an extracellular network of BMP antagonists that prevent access of BMPs to BMP receptors. *In vivo* studies in C57BL/6J mice and of transplanted GFP-labeled Sca-1^{+}CD45^{-}CD11b^{-} MSCs into bone marrow cavity of *Rag2*$^{-/-}$ immunodeficient mice showed PTH-enhanced phosphorylation of Smad1 and increased commitment of MSCs to osteoblast lineage, respectively. These data demonstrate that PTH-enhancement of MSCs differentiation to the osteoblast lineage occurs through a PTH and LRP6 dependent pathway by endocytosis of LRP6/PTH1R complex, allowing enhancement of BMP signaling.

[*] Corresponding author: Xu Cao, Ross Building, Room 229, 720 Rutland Avenue, Baltimore, MD 21205, Telephone: (410) 502-6440, Fax: (410) 502-6239, xcao11@jhmi.edu.

Supplemental material has been included.

Disclosure
All authors state that they have no conflicts of interest.

Keywords

PARATHYROID HORMONE; BONE MORPHOGENETIC PROTEINS; DIFFERENTIATION; MESENCHYMAL STEM CELLS; LOW-DENSITY LIPOPROTEIN RECEPTOR-RELATED PROTEIN 6

Introduction

Adult stem cells maintain the potential to self renew and differentiate, processes critical to tissue remodeling and repair. The decision to self renew or differentiate is regulated by the cellular microenvironment and systemic factors (1, 2). In bone remodeling, the mesenchymal stromal/stem cell (MSC) differentiates into osteoblasts, chondrocytes, or adipocytes based on changes in the microenvironment of MSCs in the bone marrow (3-5). Recent clinical data suggests that a component of osteoporosis is inadequate anabolism due to an insufficient supply of osteoblasts (6, 7). The prevention of osteoporosis is dependent on an equal balance of catabolism and anabolism such that segments of bone that are removed by osteoclasts in the resorption phase of the remodeling cycle are replaced by equivalent amounts of new bone formed by osteoblasts recruited to the same site (8) and is therefore dependent on an adequate supply of osteoblasts.

PTH is classically regarded as the primary regulator of calcium homeostasis but also has been shown to enhance bone remodeling with both anabolic and catabolic effects, dependant on intermittent or continuous administration, respectively (9-11). PTH administered once daily is currently the only anabolic drug FDA approved for treatment of osteoporosis (12). However, the precise mechanisms of how intermittent PTH results in bone formation remain elusive. PTH binds to a specific seven-transmembrane G-protein coupled receptor, PTH type 1 receptor (PTH1R). PTH1R then activates either $G\alpha_s$ or $G\alpha_q$, leading to the production of cAMP for activation of protein kinase A, or stimulation of phospholipase for protein kinase C activation, respectively (13, 14). PTH has been shown *in vitro* to enhance differentiation of MSCs into the osteoblast lineage (15), but the traditional signaling pathway of PTH does not seem to provide a satisfactory explanation for these anabolic effects. Accumulated evidence indicates that PTH anabolic effects instead result from the orchestration of the effects of local factors such as bone morphogentic proteins (BMPs), Wnts, or transforming growth factor beta (TGFβ) through recruitment of their receptors to PTH1R and/or endocytosis (16-18). For example, PTH can induce endocytosis of a PTH1R/TGFβ type II receptor (TβRII) complex (19), resulting in spatial and temporal integrated coupling of bone resorption and formation.

BMPs are expressed within the bone marrow stroma and are the only known morphogens that are able to induce osteoblast and chondroblast differentiation from MSCs (4, 5). Upon ligand binding, BMP type II receptor recruits type I receptor to form a complex and mediates type I receptor phosphorylation. Subsequently these bind with Co-Smad (Smad4) in the cytoplasm and the R-Smad-Co-Smad complex translocates to the nucleus, where it acts as either an activator or repressor for transcription of target genes (20, 21). More than 20 members of BMPs have been shown to transduce their signaling through common BMP receptors (BMPR) (3-5) resulting in altered fates of MSCs (22). BMP2 has specifically been shown to be a potent inducer of osteoblast differentiation in MSCs (3). The activity and specificity of different BMP ligands are controlled by various extracellular antagonists that regulate the binding of BMPs to their receptors. These various extracellular antagonists, such as noggin, sclerostin, Sog/Chordin (Sog/Chd) and DAN family members, are likely contributing to the diversified effects observed with BMP signaling pathways in relation to

stem cell fate (23, 24) as they bind to BMPs directly or indirectly through other extracellular proteins to prevent BMPs from gaining access to their receptors (25, 26).

Signals that eradicate the antagonist extracellular network may increase the access of BMPs to their receptors, thereby promoting differentiation of MSCs to the osteoblast lineage. We hypothesized that one mechanism of PTH-enhanced differentiation of MSCs into the osteoblast lineage is through enhancement of BMP signaling by modifying the extracellular signaling network. Low-density lipoprotein receptor-related protein 6 (LRP6) specifically functions in the canonical wnt pathway (27) and there has been increasing evidence of cross-talk between Wnt and BMP signals at the promoter level, in the cytoplasm, and in the extracellular space (28). In the extracellular space, truncation of the LRP6 extracellular domain results in constitutive activation of the canonical wnt pathway, implying that the extracellular domain exerts an inhibitory effect on signaling through this receptor (29). LRP6 also shares common antagonists with BMPs, such as sclerostin (30, 31), and antagonists of either BMP/LRP6 pathways, such as noggin and sclerostin bind to each other with high affinity ($Kd = 2.92 \times 10^{-9}M$) (32). LRP6 has also been shown to interact with the PTH signaling pathway by directly forming a complex with PTH1R (33). Therefore, we hypothesized that LRP6 may be a key element in the communication between PTH and BMP induced differentiation of MSCs into the osteoblast lineage.

In the current study, we report that PTH increases phosphorylated Smad1 (pSmad1) in MSCs *in vitro* and *in vivo*. PTH-induced endocytosis of a LRP6/PTH1R complex results in enhancement of pSmad1. Deletion of LRP6 alone is sufficient to account for the enhancement of pSmad signaling, resulting in increased access of BMP ligands to their receptors, ultimately increasing the proportion of MSCs differentiating into the osteoblast lineage. Thus, our study demonstrates one mechanism of the anabolic action of PTH is through enhancement of the differentiation of MSCs toward the osteoblast lineage by enhancing BMP-Smad signaling in a LRP6 dependent mechanism.

Materials and Methods

Mice, cell cultures and reagents

C57BL/6J (wild-type) mice were purchased from Charles River and $Tgf\beta 1^{+/+}Rag2^{-/-}$ mice with an immunodeficient background were obtained from the Mouse Models of Human Cancers Consortium Repository, US National Cancer Institute. $Tgf\beta 1^{+/+}Rag2^{-/-}$ mice were maintained as wild-type mice and used for bone marrow cavity transplantation. $Lrp6^{flox/flox}$ mice used for $Lrp6^{flox/flox}$ MSCs isolation were obtained from Van Andel Research Institute. All animals were maintained in the Animal Facility of the Johns Hopkins University School of Medicine. The experimental protocol was reviewed and approved by the Institutional Animal Care and Use Committee of the Johns Hopkins University, Baltimore, MD, USA. GFP-labeled mouse adult MSCs were obtained from the Texas A&M Health Science Center College of Medicine Institute. Cells (Passage 2) were then maintained in Iscove's modified Dulbecco's medium (IMDM, Invitrogen) supplemented with 10% fetal calf serum (FCS, Atlanta Biologicals), 10% horse serum (HS, Thermo Scientific), and 1% penicillin-streptomycin (PS, Mediatech). HEK293, UMR106, and C2C12 cells were maintained in Dulbecco's modifield Eagle's medium (DMEM, Mediatech) with 10% fetal bovine serum (FBS, Atlanta Biologicals) and 1% PS. All reagents, including plasmids, antibodies, ligands and adenoviruses, are listed in Supplemental Material.

Transfections, immunoblotting, co-immunoprecipitation, luciferase reporter assays and knockdown experiments

Transfections of DNA plasmids were performed with Lipofectamine (Invitrogen) using the protocol recommended by the manufacturer. For immunoblotting against phospho-antibodies, cells were harvested after starvation for 12-20 hours. For colocalization assays, HEK293-YFP-BMPRII and HEK293-CFP-PTH1R cells were generated by stable expression of YFP-BMPRII and CFP-PTH1R with retrovirus. Immunoprecipitation and immunoblotting analysis of cell lysates were performed as described previously (33). Luciferase activities were assayed with the Dual-Luciferase assay kit (Promega) following the manufacturer's instructions. Luciferase activity was measured and normalized to internal controls as Renilla luciferase units (RLU). β-arrestin1/2 and LRP6 knockdown experiments were performed as described in Supplemental Material.

Immunofluorescence colocalization assay

For BMPRII and PTH1R colocalization assays, HEK293 cells expressing YFP-BMPRII or CFP-PTH1R were seeded and treated with PTH^{TMR} at 37°C for indicated times and specific concentrations as reported in results section. For PTH1R internalization assays after β-arrestin 1/2 knockdown experiments, C2C12 cells expressing CFP-PTH1R were transfected with specific β-arrestin1/2 siRNA (Santa Cruz). Cells were treated with or without 100 nM PTH at 37 °C for 30 minutes after a 48 hour transfection interval. All cells were washed and fixed with 4% paraformaldehyde. Cells were mounted and observed with Zeiss LSM 510 Meta Confocal Microscope. YFP-BMPRII and CFP-PTH1R were imaged in green; PTH^{TMR} was imaged in red.

LRP6 internalization assay

For VSVG-LRP6 internalization assays, HEK293 cells were transfected with VSVG-LRP6 and Mesd. After transfection for 24 hours, cells were incubated with 100 nM PTH^{TMR} at 37 °C for 30 minutes. After the internalization of VSVG-LRP6, the cells were washed three times with cold PBS to stop endocytosis and fixed with 4% paraformaldehyde. Cells were stained with FITC-conjugated anti-VSVG antibody (Abcam) and observed with Zeiss LSM 510 Meta Confocal Microscope. LRP6 cell surface distribution was also monitored by biotinylation of cell surface proteins as described previously (34). After biotin labeling, cell lysates were immunoprecipitated with anti-LRP6 antibody and the immunoprecipitates were analyzed by immunoblotting with anti-LRP6 antibody (total LRP6) or streptavidin-HRP (cell surface LRP6). LRP6 internalization assays with flow cytometry were employed as described in Supplemental Material.

Ligand cell surface binding assay

BMP2 was labeled with ^{125}I (2000Ci/mmol) using the chloramines-T method as described for cell surface binding assays (35). For non-radioligand binding assays, BMP2 was labeled with Alexa 647 using Alexa Fluor® microscale labeling kit (Invitrogen). GFP-labeled Sca-$1^{+}CD45^{-}CD11b^{-}$ MSCs (2×10^5 cells/well) were plated in 6-well plates. After cells reached confluence, cells were washed with PBS and incubated with 250 ng/ml Alexa 647-BMP2 with or without 100 nM PTH at 37 °C for 30 minutes, then followed by another incubation at 4 °C for 4 hours. Cells were rinsed with HBAH (0.5 mg/ml BSA, 0.1% NaN3, 20 mM HEPES, pH 7.0) six times and analyzed with flow cytometry.

Biotinylation of cell surface BMPRII

HEK293 cells were transfected with various plasmids and then cell surface proteins were labeled with 0.5 mg/ml Sulfo-NHS-LC-Biotin (Thermo Scientific) at 4 °C for 1 hour. After incubation, non-binding biotin was quenched with 0.1 M glycine, followed by three washes

in cold PBS. Cells were harvested in modified RIPA (Radio-ImmunoPrecipitation Assay) buffer. Flag-BMPRII was immunoprecipitated with anti-Flag antibody and protein G sepharose (Sigma-Aldrich). Total protein and biotinylated BMPRII were analyzed by immunoblotting.

Alkaline phosphotase activity, mineralization, and CFU-F and CFU-Ob assays

For alkaline phosphotase activity and mineralization assays, GFP-labeled Sca-1^{+}CD45^{-} CD11b^{-} cells were plated on 6-well plates at a density of 2×10^5 cells/well and cultured in osteogenic medium containing 10^{-7} M dexamethasone (Sigma-Aldrich), 10 mM β-glycerol phosphate (Sigma-Aldrich), and 50 μg/ml L-ascorbic acid (Sigma-Aldrich). 100 nM PTH, or 50 ng/ml BMP2 and/or 50 ng/ml noggin were presented from day 1 to day 7 and thereafter with each change of osteogenic medium for the entire culture period. Histochemical staining for alkaline phosphotase (ALP) activity in the cells was performed using Fast BCIP/NBT Tablets (Sigma-Aldrich) according to the manufactuer's protocol at day 7 and 14. Alizarin Red staining for calcium deposits was performed at day 21. Colony forming unit-fibroblast (CFU-F) and colony forming unit-osteoblast (CFU-Ob) assays were performed as previously described (36).

Isolation and culture of Sca-1^{+}CD45^{-}CD11b^{-} MSCs

Bone marrow nucleated cells were isolated from 6-week-old *Lrp6$^{flox/flox}$* mice euthanized by cervical dislocation. Cells were cultured with Minimum Essential Medium alpha (α-MEM, Mediatech, Inc.) supplemented with penicillin (100 U/ml, Sigma-Aldrich), streptomycin sulfate (100 mg/ml, Sigma-Aldrich), and 10% fetal bovine serum (FBS, Atlanta Biologicals) at 37 °C in a 5% CO2 humidified incubator. After 72 hours of adhesion, nonadherent cells were discarded and adherent cells were cultured an additional 7 days with a single media change. The adherent cells were harvested and incubated at 4 °C for 20 minutes with PE-conjugated anti-Sca1, PerCP-conjugated anti-CD45, APC-conjugated anti-CD11b antibodies and sorted by FACSAria (Becton Dickinson). The sorted Sca-1^{+}CD45^{-}CD11b^{-}*Lrp6$^{flox/flox}$* MSCs were enriched by further culture. A similar procedure was performed on GFP-labeled MSCs to sort GFP-labeled Sca-1^{+}CD45^{-} CD11b^{-} MSCs.

PTH single injection and bone marrow cavity transplantation

For the PTH single injection model, forty 2-month-old C57BL/6J male mice were randomly divided into four groups and each group was subcutaneously administered with PTH(1-34) (Bachem, Inc., 40 μg/kg) or vehicle (equivalent volume of 1 mM acetic acid in PBS) once and were euthanized at the indicated time points after injection ($n = 10$). For bone marrow cavity transplantation model, 2-month-old C57BL/6J (wild-type) mice with an immunodeficient background (*Rag2$^{-/-}$*, male) were used as recipients. A total number of 5×10^5 GFP-labeled MSCs were injected into the bone marrow cavity of the femora as previously described (37). After treatment of vehicle or PTH at indicated times, whole bone marrow cells were harvested and incubated with antibodies listed in Supplemental Material. Expression of markers were analyzed on FACSCalibur flow cytometer (Becton Dickinson) and analyzed with Flowjo 7.6 software (Tree Star). All FACS data were analyzed with two channels, FL-1(GFP) for GFP labeled MSCs and FL-2(PE) for all other receptors or markers. Cells were gated based on FL-1 channel into a GFP positive subset. The expression of all other receptors or markers on a GFP positive subset were further presented with one-parameter histogram in FL2(PE).

Histochemistry, immunohistochemistry and histomorphometric analysis

Standard protocols were performed. Details of procedures are described in Supplemental Material.

Statistical analysis

All experiments were repeated at least three times and data are presented as mean ± the standard error of the mean (SEM). Data were analyzed using an analysis of variance or Student's t-test. $p < 0.05$ was considered statistically significant in all calculations.

Results

PTH promotes phosphorylation of Smad1 in MSCs *in vivo*

To confirm findings from prior studies (38) in which intermittent PTH administration in ovariectomized mice induced rapid phosphorylation of BMP2 target Smad1/5/8 in the periosteum, C57BL/6J wild type mice were injected with a single dose of PTH and sacrificed at 0, 30 minute, 2 hour or 8 hour after injection. A single PTH injection resulted in an increased percentage of osteoblast-like cells with phosphorylation of Smad 1/5/8 at all time points (described as phosphorylation of Smad1 or pSmad1 following). The highest percentage of osteoblast-like cells with pSmad levels occurred 30 minutes post-injection. The phosphorylation of Smad persisted for up to 8 hours post-injection as pSmad activity remained statistically significantly elevated compared to baseline activity 2 and 8 hours after a single PTH injection. (Figure 1A and 1B). To specifically examine whether PTH could induce phosphorylation of Smad1 in MSCs, GFP-labeled Sca-1^{+}CD45^{-}CD$11b^{-}$ MSCs (Supplemental Figure S1) were transplanted in the femur cavities of immunodeficient *Rag2*$^{-/-}$ mice for 3 days. A single PTH injection or vehicle was administered and bone marrow was harvested 30 minutes post-injection. FACS analysis for GFP and pSmad1 demonstrated a six fold increase in phosphorylation of Smad1 with a single PTH injection compared to vehicle, increasing pSmad1^{+} MSCs from 11.93% to 71.81% (Figure 1C and 1D). These results suggest that one step in the mechanism of PTH-promoted differentiation of MSCs to osteoblasts is through PTH-enhancement of phosphorylation of Smad1.

PTH antagonizes inhibition effect of noggin on phosphorylation of Smad1

Western blot analysis showed that PTH enhanced BMP-stimulated phosphorylation of Smad1 in a concentration and time dependent manner in UMR106 cells (Figure 2A and 2B). PTH also enhanced BMP-stimulated phosphorylation of p38, another downstream target of the BMP signaling pathway (Figure 2C). In the presence of noggin, a well known extracellular BMP antagonist, BMP-stimulated phosphorylation of Smad1 was nearly completely diminished, but recovery was seen with PTH treatment, equivalent to levels of BMP-stimulated phosphorylation of Smad1 not in the presence of noggin in C2C12 cells and MSCs (Figure 2D and 2E, respectively). Using the PTH1R-null osteocytic cell line OC59, the effect of PTH on BMP-stimulated phosphorylation of Smad1 was also abolished (Figure 2F). Collectively, these data indicate that PTH enhances BMP-stimulated phosphorylation of Smad1 through modulation of BMP signaling at the extracellular or receptor level in a PTH1R-dependent manner.

Endocytosis of LRP6 mediates PTH-enhanced phosphorylation of Smad1 in Sca-1^{+}CD45^{-}CD$11b^{-}$ MSCs

Extracellular BMP antagonists such as sclerostin and DKK1 (39) bind to the large extracellular domain of LRP6 containing 1351 animo acids to form an inhibitory network in regulating multiple signaling pathways, such as the canonical Wnt signaling pathway (40). To test the hypothesis that LRP6 may also have an inhibitory effect on the BMP signaling

pathway, phosphorylation of Smad1 in the presence or absence of BMP2 in UMR106 with knockdown of LRP6 using siRNA was assessed. Compared to scrambled siRNA, knockdown of LRP6 enhanced phosphorylation of Smad1 30 minutes after treatment with BMP2, while treatment with PTH in the absence of LRP6 no longer resulted in further increases in pSmad1 (Figure 3A and Supplemental Figure S2). Next, to test if this effect was also present in MSCs and affected by PTH signaling, Sca-1^{+}CD45^{-} CD11b^{-} MSCs were isolated from bone marrow of *Lrp6*$^{flox/flox}$ mice in which the LRP6 gene was deleted by adenovirus-mediated expression of Cre, then stimulated *in vitro* with PTH. Similar to the results in UMR106 cells, deletion of LRP6 elevated the level of pSmad1 in both the vehicle or PTH treated LRP6 deficient MSCs compared to their respective controls but PTH treatment failed to further enhance pSmad1 levels without LRP6 (Figure 3B). As PTH1R has been shown to downregulate the activity of other receptors such as TβRII via endocytosis (19), we next examined whether the observed LRP6 dependent PTH-enhanced BMP signaling was a result of endocytosis of LRP6. HEK293 cells were transfected with LRP6 plasmid and treated with vehicle or PTH. The level of cell surface LRP6 was analyzed via colocalization, cell-surface biotinylation, and FACS analysis. PTH rapidly decreased the cell surface level of LRP6 (Supplemental Figure S3A and B), indicating PTH-induced endocytosis of LRP6. Moreover, immuno-colocalization experiments demonstrated that PTH^{TMR} co-localized with LRP6 in the presence of PTH1R and internalization of the co-localized complex of LRP6 occurred within 5 minutes of administration of PTH^{TMR}. The internalization of LRP6 was not observed without expression of PTH1R, indicating that PTH induced internalization of LRP6 is PTH1R-dependent (Figure 3C). Consistent with these results, cell-surface biotinylation showed that PTH decreased endogenous cell-surface LRP6 significantly at 30 minutes in UMR106 cells (Figure 3D), but not in PTH1R-deficient OC59 cells (Supplemental Figure S4). The cell surface expression of both PTH1R and LRP6 was also statistically significantly decreased 30 minutes after PTH injection in transplantation of MSCs by FACS analysis compared to cells injected with vehicle (Figure 3E-H).

β-arrestin is a key mediator of PTH1R endocytosis (41-43). Therefore, we examined whether blockade of PTH1R endocytosis by decreasing β-arrestin could antagonize the PTH effect on phosphorylation of Smad1. Knockdown of β-arrestin using siRNA decreased both PTH-induced PTH1R endocytosis (Figure 4A) and PTH signaling downstream phosphorylation of ERK (Figure 4B). In the presence of β-arrestin, PTH enhanced pSmad1 in BMP treated cells (Figure 4C, column 2 vs column 3, $p < 0.05$). However, in the absence of β-arrestin, phosphorylation of Smad1 was not enhanced by PTH treatment (Figure 4C, column 5 vs column 6, N.S.). Similarly, treatment with chlorpromazine (CP), an endocytosis inhibitor (44), also inhibited PTH-enhanced phosphorylation of Smad1 in C2C12 cells (Figure 4D) and MSCs (Figure 4E). These results suggest that BMP stimulated phosphorylation of Smad1 is independent of β-arrestin, however PTH-enhancement of pSmad is dependent on β-arrestin, confirming that PTH-triggered endocytosis of the PTH1R/LRP6 complex is one mechanism of PTH-enhanced phosphorylation of Smad1.

Endocytosis increases the access of BMPs to receptors

We then sought to examine how PTH-induced endocytosis of PTH1R/LRP6 was enhancing BMP2 stimulated phosphorylation of Smad1. Confocal imaging for YFP-BMPRII (green color) and PTH^{TMR} (red color) in HEK293 cells showed that PTH did not induce endocytosis of BMPRII after PTH treatment (Figure 5A). Similarly, GFP-labeled Sca-1^{+}CD45^{-}CD11b^{-} MSCs that were transplanted into femur cavities of immunodeficient *Rag2*$^{-/-}$ mice did not demonstrate any affect of the cell surface level of BMPRII after PTH treatment compared to vehicle by FACS analysis (Figure 5B and 5C). However, cell-surface protein biotinylation demonstrated that knockdown of LRP6 increased the exposure of

endogenous cell-surface BMPRII significantly in C2C12 cells (Figure 5D). 125I labeled BMP2 (^{125}I-BMP2) incubated with cells in the presence or absence of PTH demonstrated that PTH significantly enhanced cell surface binding of ^{125}I-BMP2 in a dose- and time-dependent manner (Figure 5E and 5F, respectively). Similar results of increased binding of BMP2 to its receptor in the presence of PTH were seen in Sca-1^{+}CD45^{-}CD11b^{-} MSCs (Figure 5G). These results provide further evidence that PTH-induced endocytosis of PTH1R/LRP6 increases the binding of BMP2 to BMP receptors.

PTH-enhanced BMP signaling stimulates commitment of Sca-1^{+}CD45^{-}CD11b^{-} MSCs to osteoblast differentiation

To examine the effects of PTH-enhanced phosphorylation of Smad1 on lineage commitment of GFP-labeled Sca-1^{+}CD45^{-}CD11b^{-} MSCs, we seeded suspensions of MSCs at clonal density to obtain discrete colonies (CFU-F) that were treated with various combinations of BMP2, PTH, and noggin. None of the treatments exerted significant effects on the formation of CFU-Fs (Figure 6A and 6B). However, inducing the CFUs with osteogenic medium and assessing for calcium deposition (CFU-Ob) demonstrated significantly increased CFU-Obs with BMP2 (Figure 6C, column 3). PTH further increased the BMP2-induced CFU-Obs significantly (Figure 6C, column 4). Interestingly, when noggin was added to either culture condition, this effect was almost abrogated, decreasing levels below baseline control and implying alternative signaling mechanisms beyond those explored in our study. However, in the presence of BMP2 and noggin, PTH-enhanced MSCs osteogenic differentiation in CFU-Obs increased to the control levels (Figure 6A and 6C, column 6). These data are consistent with previous results (Figure 2D and 2E). Similar results were observed in the measurements of the effects of PTH on alkaline phosphatase activity and mineralization of MSCs (Supplemental Figure S5). To further confirm whether PTH-enhanced BMP signaling contributed to osteoblast differentiation of MSCs *in vivo*, GFP-labeled Sca-1^{+}CD45^{-}CD11b^{-} MSCs were transplanted into femur marrow cavity of *Rag2*$^{-/-}$ mice with injection of vehicle or PTH once daily for one week (Figure 6D). The bone marrow was harvested for FACS analysis. Osterix^{+} GFP labeled MSCs were increased from 25.52% to 44.81% in the PTH-injected mice relative to vehicle-injected group, further indicating that PTH induces osteoblast differentiation of MSCs *in vivo* (Figure 6E and 6F). Furthermore, immunostaining of osterix in GFP labeled MSCs indicated that PTH can promote osteoblast differentiation of MSCs on bone surface (Supplemental Figure S6). Altogether, these results demonstrate that one mechanism of PTH promotion of osteoblast differentiation from MSCs is through enhancement of BMP2 signaling by endocytosis of a PTH1R/LRP6 complex, resulting in increased binding of BMP2 to its receptor.

Discussion

The capacity of MSCs self-renewal and multipotency is maintained in the bone marrow microenvironment (45, 46). The decision of adult stem cells to differentiate is regulated by signals from the microenvironment. BMPs play a critical role in control of differentiation of MSCs to specific lineages including osteoblasts (47, 48), chondrocytes (49) and adipocytes (50). The activation of BMP signaling is tightly tempered by a family of soluble, extracellular secreted BMP antagonists (23) and is often integrated with other signaling pathways depending on cellular context (51-53). BMP antagonists including noggin and sclerostin act as central regulators of many complex cellular events through interaction with multiple molecular targets such as LRP6 (30). It is known that these BMP antagonists are involved in activation of both the Wnt signaling cascade (54, 55) and the BMP signaling pathways (24) required for the maintenance of MSCs in the bone marrow. In this study, we observed inhibition of BMP signaling induced by noggin in C2C12 cells and MSCs. This

inhibition was antagonized when PTH was added, resulting in enhancement of pSmad1 signaling via BMP2.

Our data also showed PTH-enhancement of pSmad signaling through an endocytic process. Endocytosis plays a critical role in initiating and spreading signals by determining which specific sub-pathway to activate or to terminate based on the internalization of plasma membranes, cell-surface receptors, and diverse soluble molecules. In some systems, the very outcome of cell signaling depends on how the various components of the signaling machinery are integrated and trafficked. For PTH signaling, β-arrestin2 mediates endocytosis of PTH1R via clatherin-coated pits, which not only mediates desensitization of G protein signaling but also effects the integration of different signals by inhibiting signal transduction (56). In this study, PTH-enhanced pSmad1 levels were attenuated by knockdown of β-arrestin. Simultaenously, these results were validated by decreased pERK with β-arrestin knockdown, which is downstream in the PTH signaling pathway. To further confirm the role of PTH1R endocytosis in PTH-enhanced BMP signaling pathway, both C2C12 cell lines and MSCs were treated with the endocytosis inhibitor, Chlorpromazine (CP), in combination with BMP and/or PTH and confirmed decreased pSmad1 levels.

LRP6 contains a large extracellular domain and binds to several Wnt signaling antagonists including sclerostin (30), DKK1 (57), Wise (58) and R-spondin (59). Interestingly, sclerostin is an antagonist for both Wnt and BMP signaling pathways. Additionally, we previously found that LRP6 is a key component for PTH signaling via interaction with PTH1R on the cell membrane and acts by formation of a ternary complex, containing PTH, PTH1R, and LRP6, promoting rapid phosphorylation of LRP6, resulting in the recruitment of axin to LRP6 and inhibition of GSK3 kinase activity and stabilization of β-catenin (33). Finally, both DKK1 and sclerostin act as negative regulators for PTH-induced cAMP production (60). Thus, we hypothesized that LRP6 may act as a central organizer for the extracellular antagonist network for the negative regulation of both Wnt and BMP signaling pathways. Our results indicate that PTH disrupts the LRP6-organized antagonist network by a unique mechanism, i.e. inducing endocytosis of PTH1R-LRP6-antagonist complex. PTH-induced endocytosis of PTH1R/LRP6 complex was evident by FACS analysis of cell surface LRP6, immunofluorescence colocalization of both proteins and analysis of cell surface biotinylated LRP6. Additionally, pSmad1 enhancement was seen with knockdown of LRP6 alone, but abrogated in PTH1R-deficient cells.

The exact mechanism of how LRP6 endocytosis enhances BMP signaling, whether through direct reduction of BMP antagonists or downregulation of wnt cascades via endocytosis, remains to be elucidated. Importantly, we show that deletion of endogenous LRP6 in MSCs increased the exposure of BMPRII to its ligand at the cell surface and that PTH-enhanced the binding affinity of BMP2 to its receptor in a dose- and time-dependent manner. Prior studies afford both as plausible hypotheses. Multiple interactions exist between BMP and Wnt antagonists (28-32). In embryonic stem cells, Wnt signaling inhibits BMP signaling (61). Kahlet et al has shown that the Wnt signaling pathway directly represses transcription of some genes including the osteocalcin gene mediated by Runx2 (62), directly inhibiting osteoblast differentiation. Figure 7 outlines our working model with the knowledge known to date. In bone growth and development, BMP activity is controlled tightly by many antagonists spatially and temporally. With PTH treatment, a PTH1R/LRP6 complex is formed and its endocytosis results in increased binding affinity of BMP to its receptor, which promotes BMP-Smad signaling and MSCs differentiation.

For the purpose of this study, we limited testing our hypothesis to BMP2 and noggin. BMP2 is the most effective osteoinducer among all the BMPs tested *in vitro* and *in vivo*, and of the known antagonists, noggin has been shown to have a high specificity and affinity for BMP2

(Kd=2 × 10^{-11} M) (63). Additionally, low concentrations of noggin have been shown to inhibit BMP effects dramatically (64). While our data demonstrate one mechanism of PTH-enhancement of BMP-pSmad1 signaling leading to MSCs differentiation, there are likely other factors besides BMP2 and noggin involved. Specifically, Figure 6A and 6C, 5th column shows that treatment with both BMP2 and noggin suppress CFU-Ob formation to less than when the cells were not treated with BMP2, indicating that either there is endogenous BMP production by these cells or the differentiation is occurring through a non-BMP pathway. Many other authors have examined the effects of various other BMPs on MSC proliferation and differentiation, which may be contributing to this effect. Sammons et al (65) found that a combination of BMP6, PTH, and vitamin D3 could induce osteoblast differentiation in normal human adult bone marrow-derived MSCs. Pountos et al (66) also showed that treatment of elderly human osteoporotic trabecular bone-derived MSCs differentiation to the osteoblast lineage could be enhanced with BMP-2, BMP-7, PTH, and PDGF. Therefore, it is likely that other BMPs may also play a similar role and may be explored in future research.

PTH, a systemic hormone controlling calcium homeostasis, stimulates the activities of both osteoclasts and osteoblasts and alters the microenvironment in the bone marrow. PTH stimulates bone formation when injected daily and is the only anabolic drug for the treatment of osteoporosis patients (67, 68). Intensive studies on the mechanisms by which PTH exerts its bone anabolic actions have focused on its effects on osteoblasts (17). The current study instead focuses on maintaining the supply of osteoblasts, revealing that PTH stimulates the commitment of MSCs to the osteoblast lineage by enhancing BMP signaling. In addition to producing cAMP as its downstream signaling, PTH orchestrates the signaling of other local factors in bone marrow to regulate the activities of osteoblasts or osteoblast progenitors. PTH-enhancement of BMP signaling is a part of the integration of the signaling networks of local factors for the spatial-temporal regulation of MSCs differentiation.

Supplementary Material

Refer to Web version on PubMed Central for supplementary material.

Acknowledgments

We would like to thank Dr. Bart O. Williams (Laboratory of Cell Signaling and Carcinogenesis, Van Andel Research Institute) for providing *Lrp6*$^{flox/flox}$ mice. This research was supported by NIH grant DK057501 to X.C., DK083350 to M.W. and T32DK007751 to J.C.

Authors' roles: BY, WL, and XC designed the experiments. BY, XLZ, CZY, LLX carried out the experiments and analyzed the data. MW and JC gave detailed comments on the paper. BY, JC and XC wrote the paper.

References

1. Yin T, Li L. The stem cell niches in bone. J Clin Invest. 2006; 116:1195–1201. [PubMed: 16670760]
2. Medici D, Shore EM, Lounev VY, Kaplan FS, Kalluri R, Olsen BR. Conversion of vascular endothelial cells into multipotent stem-like cells. Nat Med. 2010; 16:1400–1406. [PubMed: 21102460]
3. Katagiri T, Yamaguchi A, Ikeda T, Yoshiki S, Wozney JM, Rosen V, et al. The non-osteogenic mouse pluripotent cell line, C3H10T1/2, is induced to differentiate into osteoblastic cells by recombinant human bone morphogenetic protein-2. Biochem Biophys Res Commun. 1990; 172:295–299. [PubMed: 1699539]
4. Wang EA, Rosen V, D'Alessandro JS, Bauduy M, Cordes P, Harada T, et al. Recombinant human bone morphogenetic protein induces bone formation. Proc Natl Acad Sci U S A. 1990; 87:2220–2224. [PubMed: 2315314]

5. Chaudhari A, Ron E, Rethman MP. Recombinant human bone morphogenetic protein-2 stimulates differentiation in primary cultures of fetal rat calvarial osteoblasts. Mol Cell Biochem. 1997; 167:31–39. [PubMed: 9059979]
6. Martin RB, Chow BD, Lucas PA. Bone marrow fat content in relation to bone remodeling and serum chemistry in intact and ovariectomized dogs. Calcif Tissue Int. 1990; 46:189–194. [PubMed: 2106378]
7. Martin RB, Zissimos SL. Relationships between marrow fat and bone turnover in ovariectomized and intact rats. Bone. 1991; 12:123–131. [PubMed: 2064840]
8. Sorensen MS. Temporal bone dynamics, the hard way. Formation, growth, modeling, repair and quantum type bone remodeling in the otic capsule. Acta Otolaryngol Suppl. 1994; 512:1–22. [PubMed: 8191884]
9. Tam CS, Heersche JN, Murray TM, Parsons JA. Parathyroid hormone stimulates the bone apposition rate independently of its resorptive action: differential effects of intermittent and continuous administration. Endocrinology. 1982; 110:506–512. [PubMed: 7056211]
10. Hock JM, Gera I. Effects of continuous and intermittent administration and inhibition of resorption on the anabolic response of bone to parathyroid hormone. J Bone Miner Res. 1992; 7:65–72. [PubMed: 1532281]
11. Qin L, Raggatt LJ, Partridge NC. Parathyroid hormone: a double-edged sword for bone metabolism. Trends Endocrinol Metab. 2004; 15:60–65. [PubMed: 15036251]
12. Reeve J, Hesp R, Williams D, Hulme P, Klenerman L, Zanelli JM, et al. Anabolic effect of low doses of a fragment of human parathyroid hormone on the skeleton in postmenopausal osteoporosis. Lancet. 1976; 1:1035–1038. [PubMed: 57447]
13. Yamaguchi DT, Hahn TJ, Iida-Klein A, Kleeman CR, Muallem S. Parathyroid hormone-activated calcium channels in an osteoblast-like clonal osteosarcoma cell line. cAMP-dependent and cAMP-independent calcium channels. J Biol Chem. 1987; 262:7711–7718. [PubMed: 2438281]
14. Juppner H, Abou-Samra AB, Freeman M, Kong XF, Schipani E, Richards J, et al. A G protein-linked receptor for parathyroid hormone and parathyroid hormone-related peptide. Science. 1991; 254:1024–1026. [PubMed: 1658941]
15. Hollnagel A, Ahrens M, Gross G. Parathyroid hormone enhances early and suppresses late stages of osteogenic and chondrogenic development in a BMP-dependent mesenchymal differentiation system (C3H10T1/2). J Bone Miner Res. 1997; 12:1993–2004. [PubMed: 9421232]
16. Kousteni S, Bilezikian JP. The cell biology of parathyroid hormone in osteoblasts. Curr Osteoporos Rep. 2008; 6:72–76. [PubMed: 18778567]
17. Jilka RL. Molecular and cellular mechanisms of the anabolic effect of intermittent PTH. Bone. 2007; 40:1434–1446. [PubMed: 17517365]
18. Polo S, Di Fiore PP. Endocytosis conducts the cell signaling orchestra. Cell. 2006; 124:897–900. [PubMed: 16530038]
19. Qiu T, Wu X, Zhang F, Clemens TL, Wan M, Cao X. TGF-beta type II receptor phosphorylates PTH receptor to integrate bone remodelling signalling. Nat Cell Biol. 2010; 12:224–234. [PubMed: 20139972]
20. Heldin CH, Miyazono K, ten Dijke P. TGF-beta signalling from cell membrane to nucleus through SMAD proteins. Nature. 1997; 390:465–471. [PubMed: 9393997]
21. Attisano L, Wrana JL. Signal transduction by the TGF-beta superfamily. Science. 2002; 296:1646–1647. [PubMed: 12040180]
22. Varga AC, Wrana JL. The disparate role of BMP in stem cell biology. Oncogene. 2005; 24:5713–5721. [PubMed: 16123804]
23. Walsh DW, Godson C, Brazil DP, Martin F. Extracellular BMP-antagonist regulation in development and disease: tied up in knots. Trends Cell Biol. 2010; 20:244–256. [PubMed: 20188563]
24. Canalis E, Economides AN, Gazzerro E. Bone morphogenetic proteins, their antagonists, and the skeleton. Endocr Rev. 2003; 24:218–235. [PubMed: 12700180]
25. De Robertis EM, Kuroda H. Dorsal-ventral patterning and neural induction in Xenopus embryos. Annu Rev Cell Dev Biol. 2004; 20:285–308. [PubMed: 15473842]

26. O'Connor MB, Umulis D, Othmer HG, Blair SS. Shaping BMP morphogen gradients in the Drosophila embryo and pupal wing. Development. 2006; 133:183–193. [PubMed: 16368928]
27. He X, Semenov M, Tamai K, Zeng X. LDL receptor-related proteins 5 and 6 in Wnt/beta-catenin signaling: arrows point the way. Development. 2004; 131:1663–1677. [PubMed: 15084453]
28. Itasaki N, Hoppler S. Crosstalk between Wnt and bone morphogenic protein signaling: a turbulent relationship. Dev Dyn. 2010; 239:16–33. [PubMed: 19544585]
29. Liu G, Bafico A, Harris VK, Aaronson SA. A novel mechanism for Wnt activation of canonical signaling through the LRP6 receptor. Mol Cell Biol. 2003; 23:5825–5835. [PubMed: 12897152]
30. Semenov M, Tamai K, He X. SOST is a ligand for LRP5/LRP6 and a Wnt signaling inhibitor. J Biol Chem. 2005; 280:26770–26775. [PubMed: 15908424]
31. Winkler DG, Sutherland MK, Geoghegan JC, Yu C, Hayes T, Skonier JE, et al. Osteocyte control of bone formation via sclerostin, a novel BMP antagonist. EMBO J. 2003; 22:6267–6276. [PubMed: 14633986]
32. Winkler DG, Yu C, Geoghegan JC, Ojala EW, Skonier JE, Shpektor D, et al. Noggin and sclerostin bone morphogenetic protein antagonists form a mutually inhibitory complex. J Biol Chem. 2004; 279:36293–36298. [PubMed: 15199066]
33. Wan M, Yang C, Li J, Wu X, Yuan H, Ma H, et al. Parathyroid hormone signaling through low-density lipoprotein-related protein 6. Genes Dev. 2008; 22:2968–2979. [PubMed: 18981475]
34. Tamai K, Zeng X, Liu C, Zhang X, Harada Y, Chang Z, et al. A mechanism for Wnt coreceptor activation. Mol Cell. 2004; 13:149–156. [PubMed: 14731402]
35. Paralkar VM, Hammonds RG, Reddi AH. Identification and characterization of cellular binding proteins (receptors) for recombinant human bone morphogenetic protein 2B, an initiator of bone differentiation cascade. Proc Natl Acad Sci U S A. 1991; 88:3397–3401. [PubMed: 1849655]
36. Wu X, Pang L, Lei W, Lu W, Li J, Li Z, et al. Inhibition of Sca-1-positive skeletal stem cell recruitment by alendronate blunts the anabolic effects of parathyroid hormone on bone remodeling. Cell Stem Cell. 2010; 7:571–580. [PubMed: 21040899]
37. Tang Y, Wu X, Lei W, Pang L, Wan C, Shi Z, et al. TGF-beta1-induced migration of bone mesenchymal stem cells couples bone resorption with formation. Nat Med. 2009; 15:757–765. [PubMed: 19584867]
38. Ogita M, Rached MT, Dworakowski E, Bilezikian JP, Kousteni S. Differentiation and proliferation of periosteal osteoblast progenitors are differentially regulated by estrogens and intermittent parathyroid hormone administration. Endocrinology. 2008; 149:5713–5723. [PubMed: 18617606]
39. Mao B, Wu W, Li Y, Hoppe D, Stannek P, Glinka A, et al. LDL-receptor-related protein 6 is a receptor for Dickkopf proteins. Nature. 2001; 411:321–325. [PubMed: 11357136]
40. Li X, Zhang Y, Kang H, Liu W, Liu P, Zhang J, et al. Sclerostin binds to LRP5/6 and antagonizes canonical Wnt signaling. J Biol Chem. 2005; 280:19883–19887. [PubMed: 15778503]
41. Wang B, Bisello A, Yang Y, Romero GG, Friedman PA. NHERF1 regulates parathyroid hormone receptor membrane retention without affecting recycling. J Biol Chem. 2007; 282:36214–36222. [PubMed: 17884816]
42. Sneddon WB, Friedman PA. Beta-arrestin-dependent parathyroid hormone-stimulated extracellular signal-regulated kinase activation and parathyroid hormone type 1 receptor internalization. Endocrinology. 2007; 148:4073–4079. [PubMed: 17525124]
43. Ferrari SL, Pierroz DD, Glatt V, Goddard DS, Bianchi EN, Lin FT, et al. Bone response to intermittent parathyroid hormone is altered in mice null for {beta}-Arrestin2. Endocrinology. 2005; 146:1854–1862. [PubMed: 15705780]
44. Hartung A, Bitton-Worms K, Rechtman MM, Wenzel V, Boergermann JH, Hassel S, et al. Different routes of bone morphogenic protein (BMP) receptor endocytosis influence BMP signaling. Mol Cell Biol. 2006; 26:7791–7805. [PubMed: 16923969]
45. Bianco P, Robey PG, Simmons PJ. Mesenchymal stem cells: revisiting history, concepts, and assays. Cell Stem Cell. 2008; 2:313–319. [PubMed: 18397751]
46. Li L, Clevers H. Coexistence of quiescent and active adult stem cells in mammals. Science. 2010; 327:542–545. [PubMed: 20110496]

47. Lecanda F, Avioli LV, Cheng SL. Regulation of bone matrix protein expression and induction of differentiation of human osteoblasts and human bone marrow stromal cells by bone morphogenetic protein-2. J Cell Biochem. 1997; 67:386–396. [PubMed: 9361193]
48. Jaiswal N, Haynesworth SE, Caplan AI, Bruder SP. Osteogenic differentiation of purified, culture-expanded human mesenchymal stem cells in vitro. J Cell Biochem. 1997; 64:295–312. [PubMed: 9027589]
49. Sekiya I, Vuoristo JT, Larson BL, Prockop DJ. In vitro cartilage formation by human adult stem cells from bone marrow stroma defines the sequence of cellular and molecular events during chondrogenesis. Proc Natl Acad Sci U S A. 2002; 99:4397–4402. [PubMed: 11917104]
50. Tseng YH, Kokkotou E, Schulz TJ, Huang TL, Winnay JN, Taniguchi CM, et al. New role of bone morphogenetic protein 7 in brown adipogenesis and energy expenditure. Nature. 2008; 454:1000–1004. [PubMed: 18719589]
51. Moustakas A, Heldin CH. Non-Smad TGF-beta signals. J Cell Sci. 2005; 118:3573–3584. [PubMed: 16105881]
52. Guo X, Wang XF. Signaling cross-talk between TGF-beta/BMP and other pathways. Cell Res. 2009; 19:71–88. [PubMed: 19002158]
53. Zhang J, He XC, Tong WG, Johnson T, Wiedemann LM, Mishina Y, et al. Bone morphogenetic protein signaling inhibits hair follicle anagen induction by restricting epithelial stem/progenitor cell activation and expansion. Stem Cells. 2006; 24:2826–2839. [PubMed: 16960130]
54. Im J, Kim H, Kim S, Jho EH. Wnt/beta-catenin signaling regulates expression of PRDC, an antagonist of the BMP-4 signaling pathway. Biochem Biophys Res Commun. 2007; 354:296–301. [PubMed: 17222801]
55. Sharov AA, Mardaryev AN, Sharova TY, Grachtchouk M, Atoyan R, Byers HR, et al. Bone morphogenetic protein antagonist noggin promotes skin tumorigenesis via stimulation of the Wnt and Shh signaling pathways. Am J Pathol. 2009; 175:1303–1314. [PubMed: 19700758]
56. Lefkowitz RJ, Shenoy SK. Transduction of receptor signals by beta-arrestins. Science. 2005; 308:512–517. [PubMed: 15845844]
57. Mao B, Wu W, Davidson G, Marhold J, Li M, Mechler BM, et al. Kremen proteins are Dickkopf receptors that regulate Wnt/beta-catenin signalling. Nature. 2002; 417:664–667. [PubMed: 12050670]
58. Lintern KB, Guidato S, Rowe A, Saldanha JW, Itasaki N. Characterization of wise protein and its molecular mechanism to interact with both Wnt and BMP signals. J Biol Chem. 2009; 284:23159–23168. [PubMed: 19553665]
59. Binnerts ME, Kim KA, Bright JM, Patel SM, Tran K, Zhou M, et al. R-Spondin1 regulates Wnt signaling by inhibiting internalization of LRP6. Proc Natl Acad Sci U S A. 2007; 104:14700–14705. [PubMed: 17804805]
60. Shi C, Li J, Wang W, Cao W, Cao X, Wan M. Antagonists of LRP6 regulate PTH-induced cAMP generation. Ann N Y Acad Sci. 2011; 1237:39–46. [PubMed: 22082363]
61. Haegele L, Ingold B, Naumann H, Tabatabai G, Ledermann B, Brandner S. Wnt signalling inhibits neural differentiation of embryonic stem cells by controlling bone morphogenetic protein expression. Mol Cell Neurosci. 2003; 24:696–708. [PubMed: 14664819]
62. Kahler RA, Westendorf JJ. Lymphoid enhancer factor-1 and beta-catenin inhibit Runx2-dependent transcriptional activation of the osteocalcin promoter. J Biol Chem. 2003; 278:11937–11944. [PubMed: 12551949]
63. Zimmerman LB, De Jesus-Escobar JM, Harland RM. The Spemann organizer signal noggin binds and inactivates bone morphogenetic protein 4. Cell. 1996; 86:599–606. [PubMed: 8752214]
64. Abe E, Yamamoto M, Taguchi Y, Lecka-Czernik B, O'Brien CA, Economides AN, et al. Essential requirement of BMPs-2/4 for both osteoblast and osteoclast formation in murine bone marrow cultures from adult mice: antagonism by noggin. J Bone Miner Res. 2000; 15:663–673. [PubMed: 10780858]
65. Sammons J, Ahmed N, El-Sheemy M, Hassan HT. The role of BMP-6, IL-6, and BMP-4 in mesenchymal stem cell-dependent bone development: effects on osteoblastic differentiation induced by parathyroid hormone and vitamin D(3). Stem Cells Dev. 2004; 13:273–280. [PubMed: 15186723]

66. Pountos I, Georgouli T, Henshaw K, Bird H, Jones E, Giannoudis PV. The effect of bone morphogenetic protein-2, bone morphogenetic protein-7, parathyroid hormone, and platelet-derived growth factor on the proliferation and osteogenic differentiation of mesenchymal stem cells derived from osteoporotic bone. J Orthop Trauma. 2010; 24:552–556. [PubMed: 20736793]

67. Neer RM, Arnaud CD, Zanchetta JR, Prince R, Gaich GA, Reginster JY, et al. Effect of parathyroid hormone (1-34) on fractures and bone mineral density in postmenopausal women with osteoporosis. N Engl J Med. 2001; 344:1434–1441. [PubMed: 11346808]

68. Orwoll ES, Scheele WH, Paul S, Adami S, Syversen U, Diez-Perez A, et al. The effect of teriparatide [human parathyroid hormone (1-34)] therapy on bone density in men with osteoporosis. J Bone Miner Res. 2003; 18:9–17. [PubMed: 12510800]

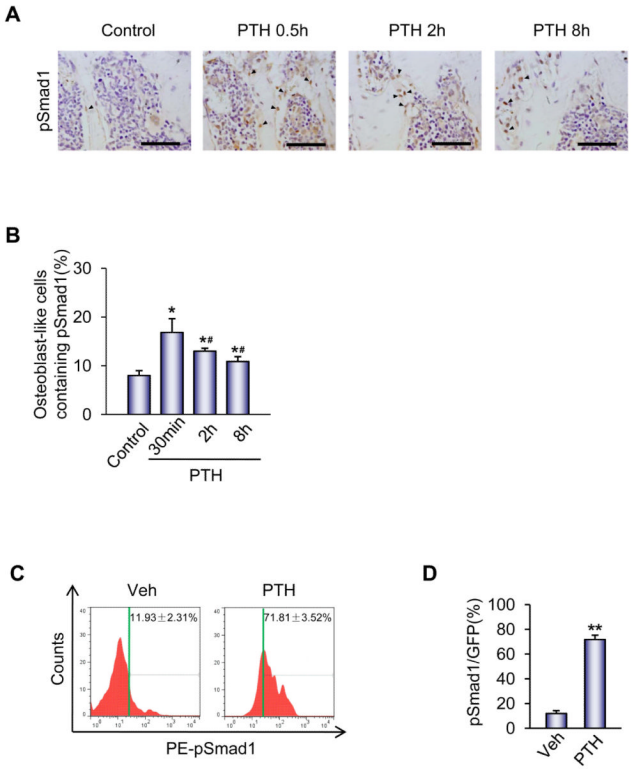

Figure 1. PTH promotes phosphorylation of Smad1 in MSCs *in vivo*

(A) Immunohistochemical analysis of phosphorylated Smad1/5/8 (pSmad1) levels in tibia sections of 2-month-old male mice at the indicated time points after a single dose injection of PTH (40 μg/kg). Arrows indicate pSmad1-positive nuclei (dark brown) in osteoblast-like cells on bone surface. Scale bars = 50 μm.

(B) Quantification of pSmad1$^+$ osteoblast-like cells is presented as percentage of total osteoblast-like cells at the indicated time points after a single dose of PTH. n=10. $^*p < 0.05$ versus control; $^\#p < 0.05$ versus 30 min time point.

(C) FACS analysis of pSmad1 levels in GFP-labeled Sca-1$^+$CD45$^-$CD11b$^-$ MSCs in mice treated with vehicle or PTH. GFP-labeled Sca-1$^+$CD45$^-$CD11b$^-$ MSCs were transplanted in the femur cavities of immunodeficient *Rag2*$^{-/-}$ mice for 3 days. Bone marrow was harvested at 30 minutes after injection of vehicle or PTH and analyzed by FACS for GFP and pSmad1.

(D) Quantification of pSmad1$^+$ GFP-labeled Sca-1$^+$CD45$^-$CD11b$^-$ MSCs is presented as percentage of GFP positive cells. n=6. $^{**}p < 0.01$ versus Veh. Data are presented as mean ± SEM.

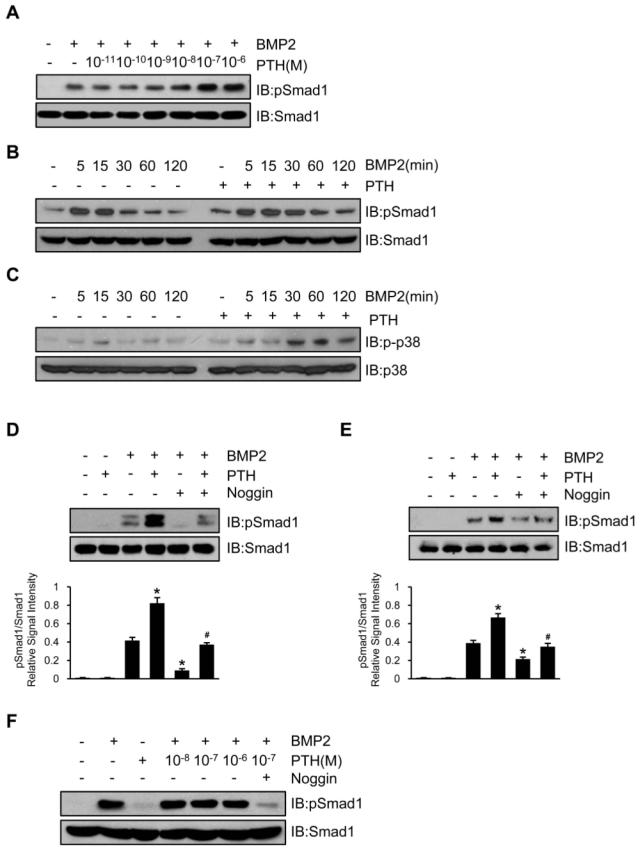

Figure 2. PTH antagonizes inhibition effect of noggin on phosphorylation of Smad1

(A,B) PTH enhanced BMP2-stimulated phosphorylation of Smad1 in a dose (A) and time (B) dependent manner in osteoblastic UMR106 cells.

(C) PTH promoted and prolonged BMP2-stimulated phosphorylation of p38 in a time-dependent manner.

(D,E) PTH enhanced BMP2-stimulated phosphorylation of Smad1 in C2C12 cells (D) and GFP-labeled Sca-1^{+}CD45^{-}CD11b^{-} MSCs (E) and noggin inhibited the effect of both as shown by Western blot analyses with Abs to phosphor-Smad1/5/8 and Smad1 with quantification by densitometry shown directly below each lane. Data are presented as mean ± SEM. $n = 3$. $^{*}p < 0.05$ versus BMP2 alone; $^{\#}p < 0.05$ versus BMP2 and noggin.

(F) PTH failed to enhance levels of pSmad1 in OC-59 PTH1R-deficient cells.

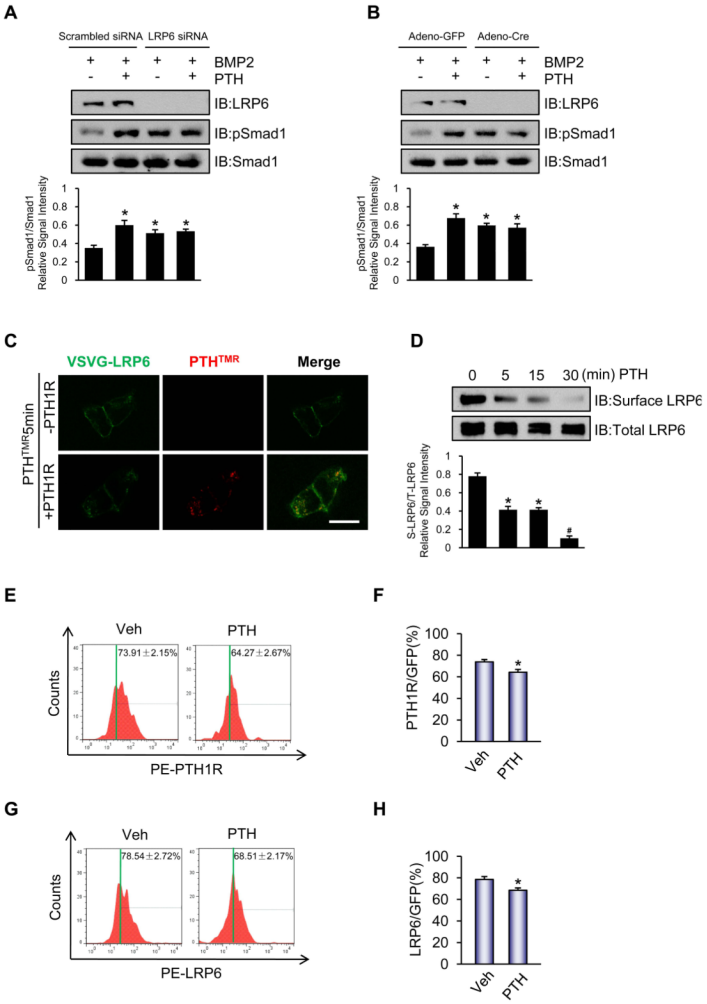

Figure 3. LRP6 mediates the inhibition of phosphorylation of Smad1 in MSCs

(A,B) Western blot analysis of pSmad1 in UMR106 cells with LRP6 siRNA knockdown (A) and in *lrp6*$^{-/-}$ MSCs performed by infection with adenovirus-mediated expression of Cre in MSCs isolated from *lrp6*$^{flox/flox}$ mice (B) after 50 ng/ml BMP2 and 100 nM PTH treatment at 37 °C for 30 minutes. Western blot analyses with Abs to LRP6, phosphor-Smad1/5/8, and Smad1 were performed. Relative phosphorylation levels of Smad1/5/8 were normalized to total Smad1 and quantified by densitometry shown directly below each lane. Data are presented as mean ± SEM. $n = 3$. $^{*}p < 0.05$ versus scrambled siRNA with BMP2 alone (A) and versus Adeno-GFP with BMP2 alone (B).

(C) PTH (red, TMR-labeled) induced endocytosis of LRP6 (green, FITC-labeled) in the presence of PTH1R (lower panels), but not in the absence of PTH1R (upper panels). LRP6 was co-localized with PTH^{TMR} during endocytosis within 5 minutes in HEK293 cells, producing a yellow color. Scale bar = 20 μm.

(D) PTH decreased cell-surface LRP6 significantly in UMR106 osteoblastic cells detected by cell surface LRP6 biotinylation analysis with quantification of data by densitometry shown directly below each lane. Data are presented as mean ± SEM. $n = 3$. $^{*}p < 0.05$ versus 0 min; $^{\#}p < 0.01$ versus 0, 5, and 15 min.

(E-H) Representative one-parameter FACS data histograms and quantification of PTH1R (E,F) or LRP6 (G,H) levels in GFP-labeled Sca-1^{+}CD45^{-}CD11b^{-} MSCs in mice treated with vehicle or PTH. GFP-labeled Sca-1^{+}CD45^{-}CD11b^{-} MSCs were transplanted in the

femur cavities of immunodeficient *Rag2*$^{-/-}$ mice for 3 days. The bone marrow nucleated cells were harvested at 30 minutes after injection of vehicle or PTH and analyzed by FACS for GFP and PTH1R (E,F) or LRP6 (G,H). Quantification data is presented as percentage of GFP positive cells and presented as mean ± SEM. $n = 6$. $^{*}p < 0.05$ versus Veh.

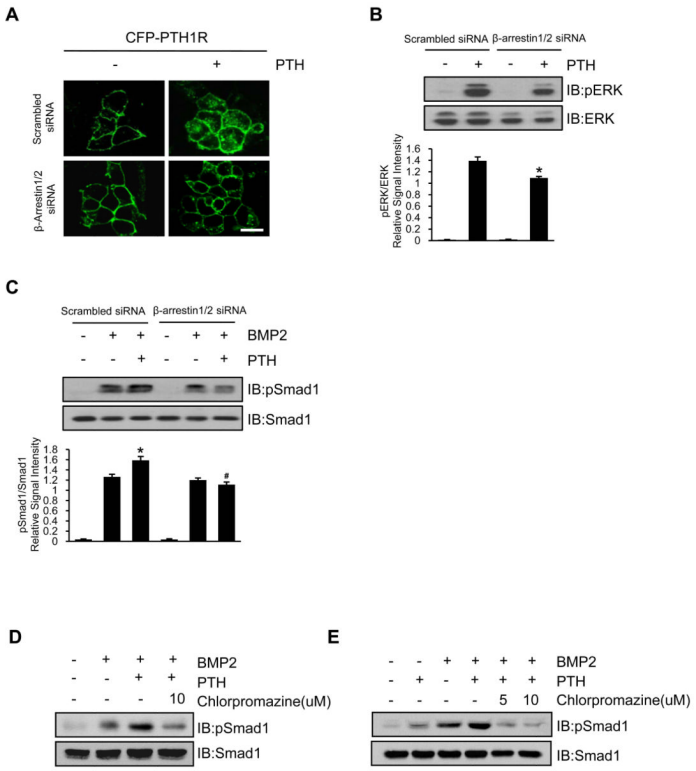

Figure 4. Inhibition of endocytosis of PTH1R antagonizes PTH-enhanced phosphorylation of Smad1

(A) Knockdown of β-arrestin by siRNA (β-arrestin1/2 siRNA) reduced PTH-induced endocytosis of PTH1R (visualized in green, CFP-labeled) in HEK293 cells. Scale bar = 10 μm.

(B,C) β-arrestin knockdown inhibited PTH-induced phosphorylation of ERK (B) and Smad1/5/8 (C) in Western blot analysis. Representative Western blot analyses with Abs to phosphor-ERK (pERK) and ERK and to phosphor-Smad1/5/8 and Smad1 were performed with quantification by densitometry comparing ratio to pERK versus total ERK (B) or pSmad versus total Smad (C) shown directly below each lane. Data are presented as mean ± SEM. $n = 3$. $^{*}p < 0.05$ versus scrambled siRNA with PTH (B) and versus scrambled siRNA with BMP2 (C). $^{\#}p < 0.05$ versus scrambled siRNA with BMP2 plus PTH.

(D,E) The endocytosis inhibitor Chlorpromazine inhibited PTH-enhanced phosphorylation of Smad1 in C2C12 cells (D) and GFP-labeled Sca-1^{+}CD45^{-}CD11b^{-} MSCs (E) by Western blot analysis.

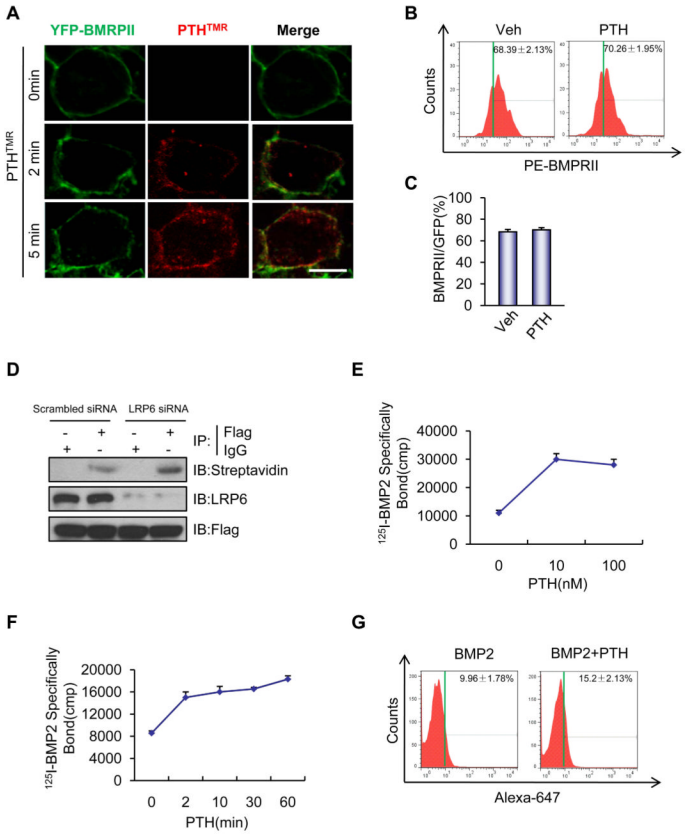

Figure 5. PTH increases the access of BMP2 to receptors by exposure of cell surface BMPRII

(A) PTH did not induce endocytosis of BMPRII. YFP-BMPRII was expressed in HEK293 cells and visualized at the cell membrane in green (left column). PTH^{TMR} (red) internalized in a time-dependent manner (middle column). No co-localization (yellow) of BMPRII-YFP expressed at membrane in green with PTH^{TMR} in red was observed after PTH treatment (right column). Scale bar = 10 μm.

(B,C) PTH did not decrease the level of cell surface BMPRII in GFP-labeled Sca-$1^{+}CD45^{-}CD11b^{-}$ MSCs harvested from the bone marrow cavity transplantation shown by representative one-parameter histograms for FASCs anaylsis (B) with quantification of BMPRII positive GFP-labeled Sca-$1^{+}CD45^{-}CD11b^{-}$ MSCs presented as percentage of GFP positive cells. Data are presented as mean ± SEM. $n = 6$.

(D) LRP6 siRNA knockdown increased cell surface exposure of BMPRII in C2C12 cells. Flag-BMPRII expression was examined using biotin-streptavidin blotting system.

(E,F) PTH stimulated cell surface binding of ^{125}I-BMP2 in a dose (E) and time (F) dependent manner in C2C12 cells. Cells were incubated with varying concentrations of PTH at 37 °C for 30 minutes (E) or with 100 nM PTH at 37 °C for varying time intervals (F). After PTH exposure, all cells were then incubated with ^{125}I-BMP2 at 4 °C for 4 hours. Data are presented as mean ± SEM. $n = 3$.

(G) PTH increased the binding of BMP2 ligand to its receptor on GFP-labeled Sca-$1^{+}CD45^{-}CD11b^{-}$ MSCs in FACS analysis. Cells were incubated with 250 ng/ml Alexa 647-BMP2 with or without 100nM PTH at 37 °C for 30 minutes, then incubated at 4 °C for 4 hours. One representative FACS analysis of three was shown.

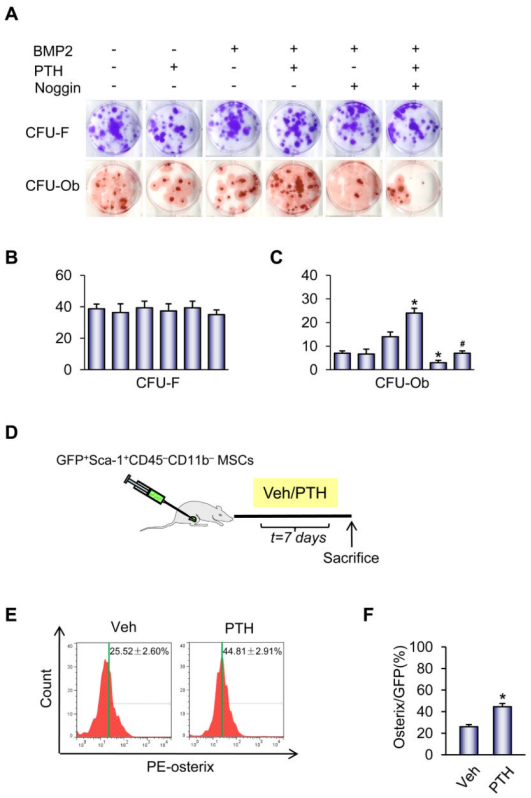

Figure 6. PTH and BMP induce commitment of GFP-labeled Sca-1^{+}CD45^{-}CD11b^{-} MSCs to osteoblast lineage

(A) Colonies formed from GFP-labeled Sca-1^{+}CD45^{-}CD11b^{-} MSCs as indicated in CFU-F and CFU-Ob assays. MSCs were plated on 6-well plates at a density of 5 cells/cm^{2} and cultured in culture medium or osteogenic medium. 100 nM PTH, 50 ng/ml BMP, and/or 50 ng/ml noggin were presented from day 1 to day 7 and thereafter with each change of culture medium or osteogenic medium for the entire culture period. The top panels show 6-well plates containing CFU-Fs stained with crystal violate. The bottom panels show 6-well plates containing CFU-Obs stained with Alizarin Red.

(B,C) The colony-forming efficiency was determined by counting the numbers of colonies. The colonies containing 50 or more cells were counted. Each bar correlates in position to treatment group of CFU-F and CFU-OB assays. $n = 3$. $^{*}p < 0.05$ versus BMP2 alone; $^{\#}p < 0.05$ versus BMP2 and noggin.

(D) Illustration of vehicle or intermittent PTH treatment for 7 days in mice with bone marrow cavity transplantation. Total number of 5×10^{5} GFP-labeled Sca-1^{+}CD45^{-}CD11b^{-} MSCs were transplanted into the femur cavity of *Rag2*$^{-/-}$ mice.

(E,F) Intermittent administration of PTH for 7 days stimulated osterix expression in GFP-labeled Sca-1^{+}CD45^{-}CD11b^{-} MSCs in representative one-parameter histogram of FACS analysis (E) and quantification (F) after transplantation. Quantification of osterix positive GFP-labeled Sca-1^{+}CD45^{-}CD11b^{-} MSCs is presented as percentage of GFP^{+} cells. $n = 6$. $^{*}p < 0.05$ versus Veh.

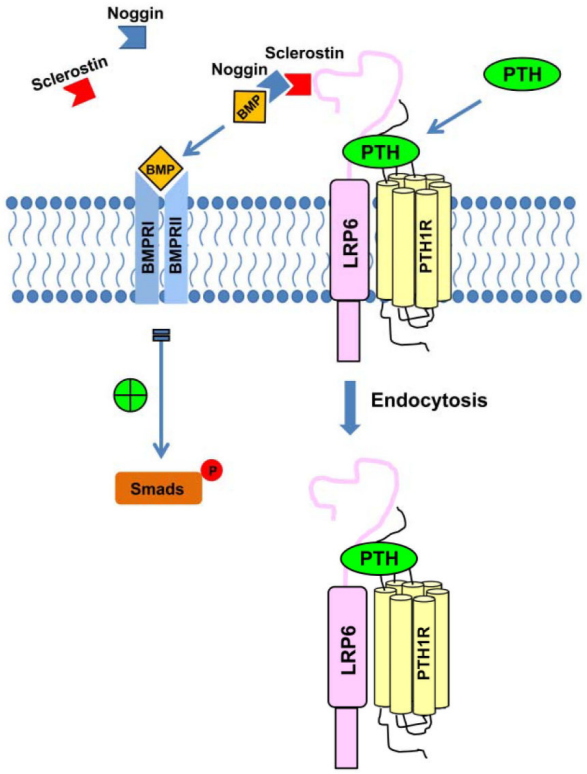

Figure 7. A schematic diagram showing the proposed actions of PTH on enhanced BMP-Smad signaling

In bone growth and development, BMP activity is controlled tightly by many antagonists spatially and temporally. With PTH treatment, a PTH1R/LRP6 complex is formed and its endocytosis results in increased binding affinity of BMP to its receptor, which promotes BMP-Smad signaling and MSCs differentiation.